Hindawi
Wireless Communications and Mobile Computing
Volume 2022, Article ID 2532905, 10 pages
https://doi.org/10.1155/2022/2532905

Research Article

Robustness-Based Transmission Strategy for Wireless-Powered Communication Networks

Xiaoying Liu, Aodi Wang, Bin Xu, Kechen Zheng, and Xinwei Yao

Zhejiang University of Technology, Hangzhou 310023, China

Correspondence should be addressed to Kechen Zheng; kechenzheng@zjut.edu.cn

Received 29 July 2022; Revised 15 September 2022; Accepted 13 October 2022; Published 25 October 2022

Academic Editor: Zhengyu Zhu

In the wireless powered communication network (WPCN), the deployed nodes that harvest energy from the power station (PS) and then transmit data to the access point (AP) may waste wireless information transmission (WIT) opportunities due to the suffered faults. Confronting this dilemma, we propose a novel metric robustness, defined as the number of available nodes for WIT, and evaluate its impact on the throughput. To optimize the tradeoff between the throughput and robustness, we design an energy threshold approach, where the robustness decreases with the energy threshold and the throughput first increases and then decreases with it due to the tradeoff between the WIT rate and WIT opportunities. In the designed approach, we formulate the nodes with different energy states as Markov chain processes and prove the existence of steady-state probability distribution. Moreover, in the scenario with high robustness by the designed approach, we select the nodes with higher energy for WIT by the improved k-means++ algorithm, in order to increase the throughput. Finally, simulations validate the theoretical analysis of the throughput and robustness performances under the improved k-means++ algorithm and show that, compared with the comparison algorithms, the improved k-means++ algorithm achieves similar throughput and robustness performances with low computational complexity.

1. Introduction

With the rapid development of the Internet of things (IoT), the number of the nodes in the world is expected to reach 30.9 billion by 2025 [1, 2]. The nodes with batteries consume energy to collect data from the environment, such as the air pressure and air quality in its sensor area, and then transmit data to the device [3–5]. However, for the nodes deployed in harsh environments, it is difficult to prevent the out-of-service events resulted from the energy depletion in the battery.

Motivated by this dilemma, researchers focus on the energy efficiency of wireless communications [6], particularly the radio frequency (RF) EH [7, 8], and the wireless-powered communication network (WPCN) that incorporates EH technology has emerged as one of the hot issues. One WPCN mode is that the nodes transmit data in the uplink by using the energy harvested from the RF signal in the downlink [9]. Compared with the conventional battery solution, there is no need to replace the batteries and the EH technology effectively enhances the sustainability of nodes in the WPCN.

Some researchers study the WPCN scenario where the nodes harvest the energy from the RF signal of the hybrid access point (HAP) in the downlink and store it in their batteries and transmit data to the HAP in the uplink when the nodes need to communicate and have the sufficient energy [10–12]. To be specific, according to the joint optimization of energy and time allocation, Lee et al. [10] maximized the throughput of the WPCN based on a dynamic time division multiple access (TDMA) approach; Song et al. [11] maximized the throughput of the WPCN based on the non-orthogonal multiple access (NOMA) transmission. By designing the transmit covariance matrices for both wireless information transmission (WET) and wireless information transmission (WIT), Jeong and Son [12] maximized the uplink capacity based on the Lagrangian method.

As the HAP plays the roles of both the access point (AP) and power station (PS), it could not receive data and transmit the RF signal simultaneously due to the hardware constraint. With the consideration about the constraint in the design of HAP, the issue of the AP and PS has become

increasingly attractive [13, 14], where the nodes transmit data to the AP in the uplink by using the energy harvested from the RF signal of the PS in the downlink. To maximize the energy efficiency, Ojo et al. [13] developed two relaying protocols by optimizing the time and power allocation and Nguyen et al. [14] developed an iterative algorithm by optimizing the time, subcarrier, and power allocation.

During the operations of the WPCN, nodes may suffer from faults and malicious attacks, especially in harsh and unattended environments, so that WIT could not occur, and the impact of the nodes' failures should be evaluated [15–18]. To be specific, Samara et al. [15] designed a detection and classification algorithm to detect the faults of nodes and Sood et al. [16] proposed a feasible approach by using the spatial correlation theory to distinguish the sensor behavior in different scenarios. To maintain the connectivity of the wireless sensor network after the nodes' failures, Wang et al. [17] proposed a central minimum cost k-connectivity restoration algorithm and Akram et al. [18] proposed a distributed movement-based algorithm.

As far as we know, few works have been done on the issues of WIT and nodes' failures in the WPCN with the AP and PS. It is difficult to repair the nodes immediately. Hence, to alleviate the impact of the nodes' failures, the number of the nodes that could be randomly selected for WIT should be increased, resulting in the decrease of the probability that WIT could not occur due to the sudden failure of the nodes.

In order to enhance the WIT when some nodes suddenly fail, we aim to improve the robustness of the WPCN, i.e., the number of the nodes that could be randomly selected for WIT, which has an impact on the throughput. To optimize the tradeoff between the throughput and robustness, we design an energy threshold approach to select the nodes that transmit the energy state information (ESI) to the AP and analyze the probability distribution of nodes' energy states by the Markov chain process. With the high energy threshold, there may not exist nodes with energy larger than the threshold to transmit the ESI, which wastes the WIT opportunity of the slot. To fully explore the WIT opportunities, we lower the energy threshold and propose the improved k-means++ algorithm to select the node from the cluster with the highest average energy (HEC) for WIT. The main contributions of this paper are summarized as follows:

(i) To reduce the failure of the WIT which resulted from the nodes' failures, we propose a novel metric *robustness*, which represents the number of the nodes that could be randomly selected for WIT. To optimize the tradeoff between the throughput and robustness, we design an energy threshold-based transmission strategy and propose the improved k-means++ algorithm to cluster the nodes with energy larger than the threshold

(ii) We formulate the energy states of nodes as the Markov chain processes and prove the existence of steady-state probability distribution for the nodes in the WPCN. Moreover, we derive the energy state transition probabilities and the achievable throughput of the WPCN

(iii) Simulation results validate the theoretical analysis of the throughput and robustness under the improved k-means++ algorithm and show that the improved k-means++ algorithm achieves similar throughput and robustness performances as comparison algorithms, while it has low computational complexity

In what follows, we present the system model in Section 2. In Section 3, we analyze the energy state of the node and the throughput of the WPCN. In Section 4, we describe the problem formulation and solution. Finally, Section 5 provides simulations to show the performances of the improved k-means++ algorithm and Section 6 concludes this paper.

2. System Model

In this section, we describe the WPCN from the network model and transmission model. The network model introduces network composition and topology. The transmission model specifies the WIT from nodes to the AP by using the energy harvested from the RF signal of the PS.

2.1. Network Model. As illustrated in Figure 1, we consider a WPCN consisting of one mobile AP, one mobile PS, and M uniformly distributed nodes, denoted by S_m, $m = 1, \cdots, M$. The WPCN area is divided into M nonoverlapping hexagons with area O, which are defined as sensor areas. Due to the limited sensing ranges of nodes, only one node is deployed in each sensor area and collects data from the sensor area. Each node is equipped with an EH device and a power conversion circuit. Only when the power of the input RF signal is larger than the predesigned threshold of the power conversion circuit that the node efficiently harvests energy from the RF signal of the PS. To characterize the area where the node successfully harvests energy, we define the harvesting zone (HZ) as a disk with radius r_e centered at the PS with respect to the path loss. Then, the number of nodes in the HZ, denoted by N_h, approximately equals $\lfloor \pi r_e^2 / O \rfloor$ where $\lfloor \cdot \rfloor$ is a floor function.

With respect to the locations of the AP and PS, there are two scenarios of the WPCN. In the first scenario, the AP is located in the HZ and $D \leq r_e$ holds, where D denotes the distance between the AP and PS. Due to the potential interference from the PS to the AP, the wireless energy transmission (WET) and WIT do not occur simultaneously. To let the AP and PS work simultaneously, we study the second scenario where the AP is located outside the HZ, i.e., $D > r_e$. Here, we do not specify the mobility models of the AP and PS and only require that the AP and PS have the same probability of being at each location [19] and the AP is located outside the HZ during the AP and PS's movements, such as the mobility model where the AP and PS move with unchanged distance. The duration of movements is relatively short compared with that of one slot and could be neglected. Then, after the AP and PS's movements, the operations of the WPCN during the rest slot are our main focus.

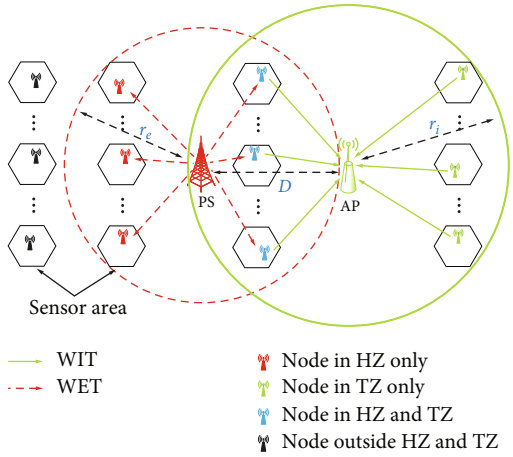

Figure 1: System model.

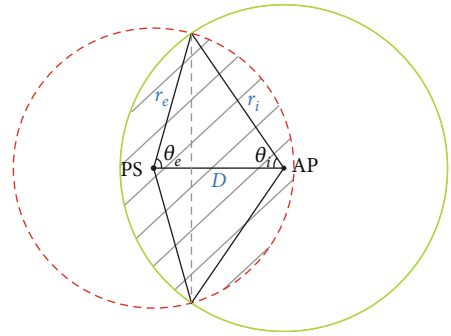

Figure 2: Topological diagram.

2.2. Transmission Model. To characterize the area where the node successfully transmits data to the AP with the path loss impact, we define the transmission zone (TZ) as a disk with radius r_i centered at the AP. The number of nodes in the TZ, denoted by N_t, approximately equals $\lfloor \pi r_i^2/o \rfloor$. As illustrated in Figure 2, the number of nodes in the overlapping area between the TZ and HZ could be given as follows:

$$N_o = \left\lfloor \frac{1}{O}\left(\theta_i r_i^2 - \frac{1}{2}r_i^2 \sin(2\theta_i) + \theta_e r_e^2 - \frac{1}{2}r_e^2 \sin(2\theta_e)\right)\right\rfloor, \tag{1}$$

where θ_i and θ_e are the angles in Figure 2, $\theta_i r_i^2 - (1/2)r_i^2 \sin(2\theta_i)$ represents the area of the segment on the left of the dotted line, $\theta_e r_e^2 - (1/2)r_e^2 \sin(2\theta_e)$ represents the area of the segment on the right of the dotted line, and $\lfloor \cdot \rfloor$ is a floor function. As illustrated in Figure 2, we have

$$\begin{aligned} r_i \cos\theta_i + r_e \cos\theta_e &= D, \\ r_i \sin\theta_i &= r_e \sin\theta_e. \end{aligned} \tag{2}$$

Based on (2), we have

$$\begin{aligned} \theta_i &= \arccos\left(\frac{r_i^2 - r_e^2 + D^2}{2Dr_i}\right), \\ \theta_e &= \arccos\left(\frac{r_e^2 - r_i^2 + D^2}{2Dr_e}\right). \end{aligned} \tag{3}$$

The WPCN adopts a synchronous slotted protocol for the AP, PS, and nodes. From the long-term perspective, we consider that each node in the HZ harvests the same amount of energy during the WET, denoted by E_u, which is viewed as the energy unit [20]. Note that the considered energy harvesting model could become more realistic if the harvested energy is further subdivided into smaller energy units based on the distance between the node and PS. Let $\{0, E_u, \cdots, \mu E_u\}$ be the set of energy states for all the nodes, where μE_u represents the battery capacity, and the node in state j has available energy jE_u. As illustrated in Figure 3, each slot, with equal duration τ, consists of three phases: channel estimation phase (CEP), node selection phase (NSP), and transmission phase (TP).

During the CEP $[0, \tau_c]$, the PS keeps idle. We divide CEP into durations with the same time span τ_s, and the nodes in the TZ transmit ESI to the AP by the TDMA protocol. Since the number of the durations in the CEP is limited, the AP may not receive the ESI from all the nodes. Therefore, we design an energy threshold approach to limit the number of the nodes that could transmit ESI. Let ξ denote the energy threshold with the unit of E_u, i.e., only the node with energy no less than ξE_u, referred to as the active node (AN), could transmit ESI to the AP. Furthermore, the node with energy less than ξE_u, which is referred to as the inactive node (IN), could not transmit ESI to the AP.

During the NSP $(\tau_c, \tau_c + \tau_n]$, the PS keeps idle. According to the received ESI, the AP has two kinds of actions. In action 1, if the AP receives the ESI, we obtain HEC by the improved k-means++ algorithm, which will be presented in Section 4. We let the AP transmit feedback information to the randomly selected node in the HEC, to inform it to be ready for the WIT during the TP. In action 2, if the AP does not receive the ESI, it keeps idle.

During the TP $(\tau_c + \tau_n, \tau]$, the nodes in the HZ, except the selected node for the WIT, harvest energy from the RF signal of the PS. Hence, in action 1, the WET occurs. If the AP does not receive data in a short duration, it considers that the node suddenly fails and it transmits feedback information to another node randomly selected from the HEC for the WIT. This process continues until the WIT occurs or the AP transmits feedback information to all the nodes in the HEC. If the AP transmits the feedback to all nodes in the HEC and still does not receive the data, we consider that the WIT failure occurs due to the sudden failure of the nodes. In action 2, only the WET occurs.

During the TP, the selected node exhausts its energy for the WIT with constant power. Based on Shannon's channel capacity, the throughput of the channel from node S_m to the AP could be given as

$$R_m = \frac{\tau_t}{\tau} \log_2\left(1 + \frac{E_m h_{m,t}}{\tau_t \sigma^2}\right), \tag{4}$$

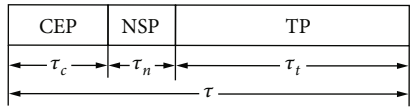

Figure 3: Slot structure.

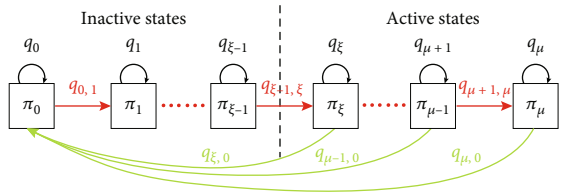

Figure 4: A Markov chain process with energy state space $\{0, E_u, \cdots, \mu E_u\}$.

where E_m denotes the energy buffered in the battery of node S_m, $h_{m,t}$ denotes the channel gain from node S_m to the AP at slot t, τ_t denotes the duration of the TP, and σ^2 denotes the power of noise. In addition, we consider the case of saturated traffic that the node has sufficient data to transmit and the throughput in (4) could be regarded as the upper bound [21].

3. Energy State Analysis of the WPCN

In this section, we first analyze the energy states of nodes by the Markov chain process, prove the existence of steady-state probability distribution for the nodes in the WPCN, and formulate the throughput of the WPCN.

3.1. Energy State. According to the transmission model in Section 2.2, there are three cases of energy state transition based on the actions of nodes. In case 1, if the node in the HZ harvests energy from the RF signal of the PS or the battery of the node is not fully charged, the energy in the node increases by E_u. In case 2, if the node is selected for the WIT, the energy of the node is exhausted for the WIT. In case 3, if the node does not transmit data or harvest energy or if the battery of the node is not fully charged, the energy of the node remains unchanged. Then, we model the probability distribution of nodes' energy states by the Markov chain process, as illustrated in Figure 4. We define π_x as the probability that the node is in state x, where x is a non-negative integer. We also define $q_{j,k}$ as the transition probability of the energy transition from state j at the current slot to state k at the next slot. If $j = k$, $q_{j,k}$ is simplified as q_j.

Theorem 1. *There is at least one steady-state probability distribution for the nodes in the WPCN.*

Proof. We employ $\pi = [\pi_0, \pi_1, \cdots, \pi_\xi, \cdots, \pi_\mu]^T$ to denote the set of energy states, and $\sum_{x=0}^{\mu} \pi_x = 1$ holds. Based on the Markov chain process in Figure 4, the matrix of energy state transition probabilities is

$$A = \begin{bmatrix} q_0 & q_{0,1} & & & & & & & \\ & q_1 & q_{1,2} & & & & & & \\ & & \ddots & \ddots & & & & & \\ & & & q_{\xi-1} & q_{\xi-1,\xi} & & & & \\ q_{\xi,0} & & & & q_\xi & q_{\xi,\xi+1} & & & \\ \vdots & & & & & \ddots & \ddots & & \\ q_{\mu-1,0} & & & & & & q_{\mu-1} & q_{\mu-1,\mu} & \\ q_{\mu,0} & & & & & & & q_\mu & \end{bmatrix}, \tag{5}$$

where the number of columns is equal to that of rows. Therefore, based on the Markov property [22], the proof is equivalent to proving that the following equation has at least one nonzero solution:

$$A\pi = \pi. \tag{6}$$

Then, we obtain another form of (6) as

$$(A - E)\pi = 0, \tag{7}$$

where E is a unit matrix with the same number of the rows and columns in A.

$$|A - E| = \begin{vmatrix} q_0 - 1 & q_{0,1} & & & & & & & \\ & q_1 - 1 & q_{1,2} & & & & & & \\ & & \ddots & \ddots & & & & & \\ & & & q_{\xi-1} - 1 & q_{\xi-1,\xi} & & & & \\ q_{\xi,0} & & & & q_\xi - 1 & q_{\xi,\xi+1} & & & \\ \vdots & & & & & \ddots & \ddots & & \\ q_{\mu-1,0} & & & & & & q_{\mu-1} - 1 & q_{\mu-1,\mu} & \\ q_{\mu,0} & & & & & & & q_\mu - 1 & \end{vmatrix}. \tag{8}$$

Then, the proof is equivalent to proving that $|A-E|$ has more rows than columns [23], where $|A-E|$ could be given as (8), shown at the top of the next page.

$$|A-E| = \begin{vmatrix} q_0 - 1 + q_{0,1} & q_{0,1} & & & & \\ q_1 - 1 + q_{1,2} & q_1 - 1 & q_{1,2} & & & \\ \vdots & & \ddots & \ddots & & \\ q_{\xi-1} - 1 + q_{\xi-1,\xi} & & & q_{\xi-1} - 1 & q_{\xi-1,\xi} & \\ q_{\xi,0} + q_\xi - 1 + q_{\xi,\xi+1} & & & & q_\xi - 1 & q_{\xi,\xi+1} \\ \vdots & & & & & \ddots \\ q_{\mu-1,0} + q_\mu - 1 + q_{\mu-1,\mu} & & & & & \\ q_{\mu,0} + q_\xi - 1 + q_{\xi,\xi+1} & & & & & \end{vmatrix} \quad \begin{matrix} \\ \\ \\ \\ \\ \ddots \\ q_{\mu-1} - 1 \\ \\ q_{\mu-1,\mu} \\ q_\mu - 1 \end{matrix} . \tag{9}$$

By adding the values of each column to the first column, (8) is rewritten as (9), shown at the top of the next page.

Based on the Markov property [22], we have the relationship among the energy state transition probabilities as

$$\sum_{j=0}^{\mu} A_{ij} = 1, \quad i = 0, 1, \cdots, \mu. \tag{10}$$

Based on (10), we find that the values of the first column in the determinant of (9) are equal to zero. Therefore, $|A-E|$ has one more column than row and we complete the proof. □

Based on the definition of the AN in Section 2.2, when the probability distribution of nodes' energy states becomes steady, the probability that the node is AN could be given as

$$P_a = \sum_{x=\xi}^{\mu} \pi_x. \tag{11}$$

Furthermore, the probability that there is no AN in the TZ could be given as

$$P_t = (1-P_a)^{N_t} = \left(\sum_{x=0}^{\xi-1} \pi_x \right)^{N_t}. \tag{12}$$

According to the ANs in the TZ, we divide the transition probability $q_{j,j+1}$ into two situations. In situation 1, if there is no AN in the TZ, the number of the nodes that harvest energy equals N_h. In situation 2, if there is at least one AN in the TZ, the analysis of the transition probability $q_{j,j+1}$ could be divided into two cases according to the location of the selected node for the WIT. In case 1, if the node selected for the WIT is deployed in the TZ but outside the HZ, the number of the nodes that harvest energy equals N_h. In case 2, if the node selected for the WIT is deployed in the overlapping area between the HZ and TZ, the number of the nodes that harvest energy equals $N_h - 1$. Therefore, the transition probability of energy transition from state j at the current slot to state $j+1$ at the next slot could be given as

$$q_{j,j+1} = \begin{cases} P_t \dfrac{N_h}{M} + (1-P_t)(P_{et} + P_{eo}), & \text{if } 0 \le j < \mu, \\ 0, & \text{if } j \ge \mu, \end{cases} \tag{13}$$

where $P_{et} = N_h/M(1-(N_o/N_t))$ represents the probability that the node harvests energy and it is deployed in the HZ; $P_{eo} = (N_h - 1)N_o/MN_t$ represents the probability that the node harvests energy and it is deployed in the overlapping area between the HZ and TZ. Then, we define positive nodes (PNs) as the nodes that could be randomly selected for the WIT. The transition probability of energy transition from state j at the current slot to state 0 at the next slot could be given as

$$q_{j,0} = \begin{cases} \displaystyle\sum_{y=1}^{N_t} \frac{1}{y} P_y, & \text{if } \xi \le j < \mu, \\ 0, & \text{if others,} \end{cases} \tag{14}$$

where $P_y = C_{N_t}^{y} \left(\sum_{x=a}^{b} \pi_x\right)^{y} \left(\sum_{x=0}^{a-1} \pi_x\right)^{N_t - y}$ represents the probability that there are y PNs in the WPCN, a denotes the lowest energy state of the PNs, b denotes the highest energy state of the PNs, and $\xi \le a \le j \le b \le \mu$ holds.

3.2. Expected Throughput Formulation. Since there is at least one AN in the TZ when the WIT occurs, the long-term expected throughput of the WPCN could be given as

$$R = (1-P_t)E(a,b), \tag{15}$$

where $E(a, b)$ represents the expected throughput during one slot when the lowest energy state of the PNs equals a and the highest energy state of the PNs equals b. Considering the probability distribution of nodes' energy states, we formulate $E(a, b)$ in (15) as

$$E(a,b) = \frac{\sum_{q=a}^{b} \pi_q Q(q)}{\sum_{p=a}^{b} \pi_p},$$
$$Q(q) = \frac{\tau_t}{\tau} \log_2\left(1 + \frac{qE_u h_t}{\tau_t \sigma^2}\right), \tag{16}$$

where $Q(q)$ represents the throughput achieved by the nodes with energy qE_u, h_t denotes the channel gain from the node to the AP at slot t, and the values of a and b vary from one slot to another.

4. Problem Formulation and Solution

In this section, we first introduce the significance and definition of robustness and propose the improved k-means++ algorithms to select the node for the WIT.

In the energy threshold approach, we optimize the energy threshold to obtain ANs and randomly select one of the ANs to transmit data to the AP. Based on the transmission model in Section 2.2, we deduce that the probability that the WIT successfully occurs during the TP increases with the robustness of the WPCN, i.e., the number of the PNs. Hence, the ANs are viewed as the PNs and we infer that the robustness of the WPCN increases with the number of ANs and decreases with the energy threshold. However, under the energy threshold approach, there is a probability that no PNs exist at some slots, indicating that the WIT does not occur, and the WIT opportunities at some slots are wasted.

To fully explore the WIT opportunities, we lower the energy threshold to increase the number of PNs. However, the decrease of the energy threshold results in the decrease of the WIT rate and throughput. To be specific, with the decrease of the energy threshold, some nodes with low energy are allocated to the PNs, which decreases the average energy of the PNs for WIT. To compensate the throughput degradation which resulted from low energy threshold, we integrate the clustering algorithm to cluster ANs and randomly select the node from the HEC for the WIT and optimize the tradeoff between the throughput and robustness.

Considering the speed and accuracy of the clustering algorithms [24], we use Algorithm 1 to cluster the ANs. Consider that there are n ANs for clustering, where $n \in [1, N_t]$ holds. Then, the cluster of observations about the values of nodes' energy states is denoted by $X = \{x_1, x_2, \cdots, x_n\}$. By Algorithm 1, we partition X into k clusters, denoted by $\{C_i | i = 1, \cdots, k\}$, to minimize the distance between observations and centers in the clusters. Since the PNs transmit data to the AP by consuming all the energy during the TP, the throughput increases with the average energy of the PNs based on (4). If the number of clusters is not limited, the nodes with the same energy state may be divided into different clusters, which results in the decrease of the number of the PNs in the HEC and the decrease of the robustness. To alleviate the problem that the nodes with the same energy state are divided into different clusters, we improve the k-means++ algorithm in line 1. To be specific, we let $k = \min\{k, N_{es,t}\}$, where $N_{es,t}$ denotes the number of energy states at slot t. In lines 2–5, the centers of the clusters are randomly selected from the observations one by one, denoted by $\{K_i | i = 1, \cdots, k\}$. The probability that the observation x is selected increases with the distance from the nearest known center to the observation. In lines 9–11, cluster C_j of observation x with state j is

$$C_j = \underset{C_i, i \in \{1, \cdots, k\}}{\operatorname{argmin}} |j - K_i|. \tag{17}$$

In lines 12–14, based on (17), we update the center K_i of the cluster C_i as

$$K_i = \frac{\Sigma_{x \in C_i} x}{|C_i|}. \tag{18}$$

The clusters of the observations in (17) and the centers in (18) are updated according to each other until the centers of the clusters do not change.

The nodes in the HEC could be viewed as the PNs, and the value of robustness equals the number of the nodes in the HEC. Then, we calculate R in (4), where E_m represents the energy of the node randomly selected from the PNs.

5. Simulations

In this section, we provide simulations to show the impacts of the improved k-means++ algorithm on the throughput and robustness of the WPCN with 100 nodes. We set the number of nodes in the TZ $N_t = 36$, the number of nodes in the HZ $N_h = 12$, and the number of nodes in the overlapping area between the TZ and HZ $N_o = 6$. For the slot structure, the duration of the TP $\tau_t = 9$ ms and the duration of the slot $\tau = 10$ ms hold. The energy state of the nodes in the WPCN belongs to the range $[0, 18]$. In addition, we consider that the average amount of the harvested energy during the TP $E_u = 10^{-5}$ Joules and the power of noise $\sigma^2 = -50$ dBm. For the simplicity of analysis, we assume that the AP receives all the ESI during the CEP and the channel gain from each node to the AP at each slot $h_{m,t} = -60$ dB.

Figure 5 plots the slot efficiency of the WPCN versus the energy threshold ξ, where the slot efficiency denotes the possibility that the WIT opportunity of the slot is not wasted. We observe that the slot efficiency remains unchanged with ξ when $\xi \in [1, 10)$ and decreases with ξ when $\xi \in [10, 18]$. The reason for the decrease of slot efficiency is that the high value of ξ results in no ANs for the WIT and wastes the WIT opportunities at some slots. Furthermore, we infer that the highest energy state of the nodes is no less than 10 at each slot in the WPCN; thus, $\xi = 10$ holds in Algorithm 1 in order to exploit the transmission opportunities.

Figure 6 plots the throughput and robustness of the WPCN versus the energy threshold ξ. We observe that the

Input: The number of clusters k, the energy states of nodes $X = \{x_1, x_2, \cdots, x_n\}$;
Output: HEC;
1: $k = \min\{k, N_{es,t}\}$;
2: Randomly select an observation as the center from X;
3: **while** the number of the centers is less than k**do**
4: Select an observation x as the center K_i from X with the probability that increases with the distance from the nearest known center to the observation;
5: **end while**
6: $l = 0, FLAG_l = 0$;
7: **repeat**
8: $l++, FLAG_l = K$;
9: **for**$j = \xi$ to μ**do**
10: According to the observation x with state j, select the cluster C_j by (14);
11: **end for**
12: **for**$i = 1$ to k**do**
13: Calculate the center K_i of the cluster C_i in (18);
14: **end for**
15: **until**$FLAG_l = FLAG_{l-1}$;
16: **return** HEC.

Algorithm 1: Improved k-means++ algorithm.

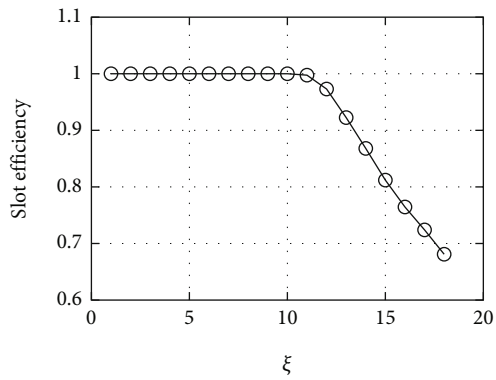

Figure 5: The slot efficiency of the WPCN versus the energy threshold ξ.

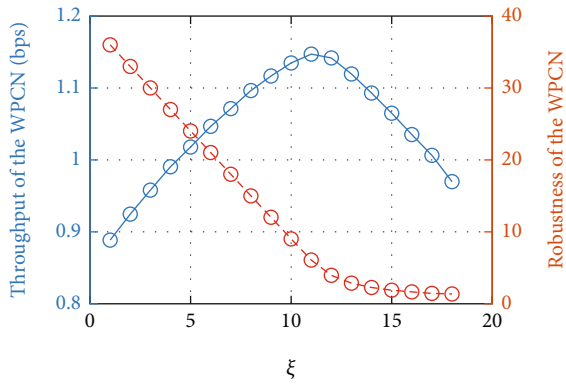

Figure 6: The throughput and robustness of the WPCN versus the energy threshold ξ, where the PN is selected from the ANs for the WIT.

throughput increases with ξ when $\xi \in [1, 11)$ and the robustness decreases with ξ when $\xi \in [1, 18]$ and these observations are in correspondence with the theoretical results in Section 4. Furthermore, when $\xi \in [11, 18]$, we observe the throughput decreases with ξ, which is due to the reason that a high value of ξ results in the decrease of the slot efficiency.

Figure 7 plots the throughput and robustness of the WPCN under Algorithm 1 and k-means++ algorithm versus the number of the clusters k, and $\xi = 10$ holds. When $k \in [1, 4)$, we observe that the throughput increases with k and the robustness decreases with k. These observations are explained as follows. With the increase of k, some of the ANs with relatively low energy would not be viewed as the PNs, which increases the average energy of the PNs. Besides, the PNs transmit data to the AP by consuming all the energy during the TP; thus, the throughput increases with the average energy of the PNs. When $k \in [4, 9]$, under Algorithm 1, we observe that the throughput and robustness remain almost unchanged with k, which is due to the reason that the ANs are divided into at most four clusters for a majority of slots based on the simulation results. However, when $k \in [4, 9]$, we observe that the throughput remains almost unchanged with k and the robustness decreases with k under the k-means++ algorithm. This observation is due to the reason that when the number of clusters exceeds the number of ANs' energy states, the ANs with the highest energy state could be distributed in different clusters, which results in the decrease of the number of the PNs, i.e., the robustness. Since the PNs transmit data to the AP by consuming all the energy during the TP, the throughput increases with the average energy of the PNs based on (4). When the number of clusters exceeds the number of ANs' energy states, the energy state of the PNs does not change with k and the throughput remains almost unchanged with k.

Figure 8 plots the throughput and robustness of the WPCN under Algorithm 1, improved k-medoids algorithm [25], improved hierarchical algorithm [26], the energy

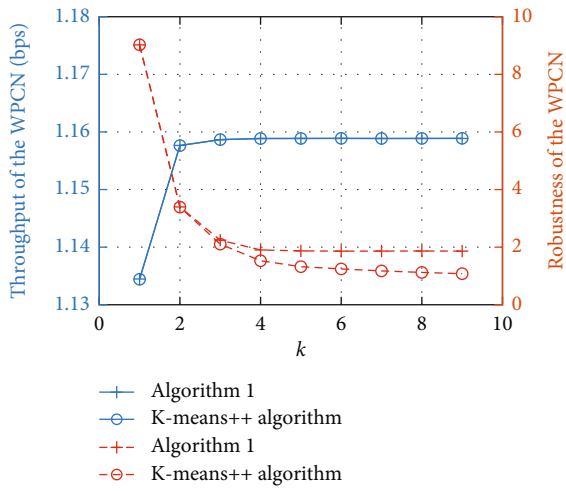

Figure 7: The throughput and robustness of the WPCN versus the number of the clusters k, where the PN is selected from the EHC for the WIT.

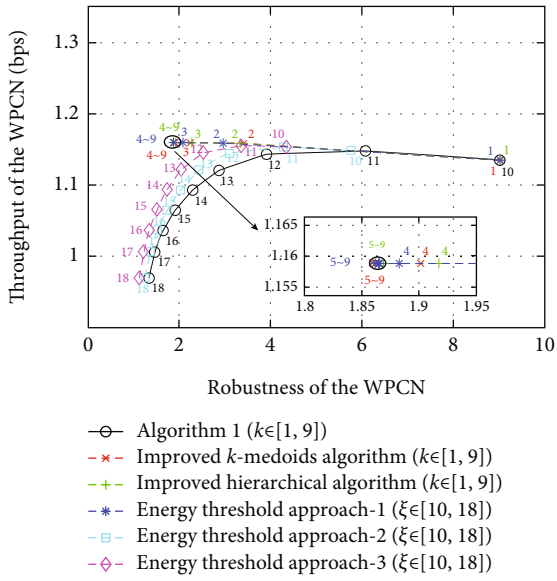

Figure 8: Comparison of throughput and robustness in the WPCN under Algorithm 1, improved k-medoids algorithm, improved hierarchical algorithm, the energy threshold approach 1, the energy threshold approach 2, and the energy threshold approach 3. In the three energy threshold approaches, the number near the point represents the value of ξ. In the other three clustering algorithms, the number near each point represents the value of k.

threshold approach-1, the energy threshold approach-2, and the energy threshold approach-3. To be specific, both improved k-medoids algorithm and improved hierarchical algorithm contain the same optimization process as Algorithm 1, where $\xi = 10$. Under energy threshold approach-1, one of the ANs is selected for the WIT, i.e., the number of the PNs equals that of the ANs. Under energy threshold approach-2, one of the one-half ANs with high energy states according to the descending order of ANs' energy states is selected for the WIT, i.e., the number of the PNs equals one-half of that of the ANs. Under energy threshold approach-3, one of the one-third ANs with high energy states according to the descending order of ANs' energy states is selected for the WIT, i.e., the number of the PNs equals one-third of that of the ANs.

We observe that Algorithm 1 achieves similar throughput and robustness performances as the improved k-medoids algorithm and improved hierarchical algorithm. In the three clustering algorithms, the throughput decreases with the robustness. The reasons for these observations are similar as those in Figures 6–7. We observe in Figure 8 that the throughput of the WPCN first increases with the robustness and then decreases with the robustness under the three energy threshold approaches. The reasons for these observations are similar as those in Figure 6. Under the same energy threshold, we observe in Figure 8 that the robustness of the WPCN under energy threshold approach-2 is smaller than that of energy threshold approach-1 and larger than that of energy threshold approach-3. The observations about the robustness are due to the reason that the number of the PNs under energy threshold approach-2 is smaller than that under energy threshold approach-1 and larger than that of energy threshold approach-3. Under the energy threshold smaller than 18, we observe that the throughput of the WPCN under energy threshold approach-2 is smaller than that under energy threshold approach-3 and larger than that under energy threshold approach-1. The observations about the throughput are due to the reason that the ANs with low energy states that could be selected as PNs under energy threshold approach-2 could not be selected as PNs under energy threshold-3, i.e., the average energy of the PNs under energy threshold approach-2 is lower than that under energy threshold approach-3. The relationship between energy threshold approach-1 and energy threshold approach-2 is similar as that between energy threshold approach-2 and energy threshold approach-3. Besides, the PNs transmit data to the AP during the TP by consuming all the energy; thus, the throughput of the WPCN under energy threshold approach-2 is smaller than energy threshold approach-3 and larger than that under energy threshold approach-1. When the energy threshold equals 18, the throughput of the WPCN under the three energy threshold approaches is the same. The observation about the throughput is due to the reason that the maximum energy state of the ANs equals 18, and the energy states of the PNs under the three energy threshold approaches are the same. Specifically, with the same robustness, the throughput of the WPCN under the three clustering algorithms is higher than that under the three energy threshold approaches.

6. Conclusion

In this paper, we studied the robustness of the WPCN, where the nodes transmit data to the AP by consuming the energy harvested from the PS. According to the theoretical analysis about the WIT, we find that the robustness has an impact on the throughput. To optimize the tradeoff between the throughput and robustness, we develop a transmission strategy with an energy threshold approach to fully explore the WIT opportunities and propose the improved k-means++ algorithm to

cluster the nodes with energy larger than the threshold to increase the throughput. Besides, we analyze the probability distribution of nodes' energy states by the Markov chain process and prove the existence of steady-state probability distribution for the nodes in the WPCN.

According to the simulations, we have four findings listed as follows: (1) with a low energy threshold, the WIT opportunities are fully explored, the throughput increases with the energy threshold, and the robustness decreases with the energy threshold. (2) With high energy threshold, the WIT opportunities are not fully explored and both the throughput and robustness decrease with the energy threshold. (3) To fully explore the WIT opportunities with low robustness, we lower the energy threshold to increase the robustness and validate that the improved k-means++ algorithm achieves higher throughput than that obtained by only the energy threshold approach. (4) The improved k-means++ algorithm, improved k-medoids algorithm, and improved hierarchical algorithm achieve similar throughput and robustness performances of the WPCN, and the improved k-means++ algorithm has the lowest computational complexity.

Data Availability

The data used to support the findings of this study are available from the corresponding author upon request.

Conflicts of Interest

The authors declare that there is no conflict of interest regarding the publication of this paper.

Acknowledgments

This work is supported in part by the National Natural Science Foundation of China, Grant numbers: 61902351 and 61902353; in part by the Zhejiang Provincial Natural Science Foundation of China, Grant numbers: LY21F020022 and LY21F020023; and in part by the Fundamental Research Funds for the Provincial Universities of Zhejiang under Grant number RF-A2022005.

References

[1] Q. Wu, X. Guan, and R. Zhang, "Intelligent reflecting surface-aided wireless energy and information transmission: an overview," *Proceedings of the IEEE*, vol. 110, no. 1, pp. 150–170, 2022.

[2] Z. Li, W. Chen, Q. Wu, K. Wang, and J. Li, "Joint beamforming design and power splitting optimization in IRS-assisted SWIPT NOMA networks," *IEEE Transactions on Wireless Communications*, vol. 21, no. 3, pp. 2019–2033, 2022.

[3] X. Liu, B. Xu, X. Wang, K. Zheng, K. Chi, and X. Tian, "Impacts of sensing energy and data availability on throughput of energy harvesting cognitive radio networks," *IEEE Transactions on Vehicular Technology*, pp. 1–13, 2022.

[4] H. Hu, K. Xiong, G. Qu, Q. Ni, P. Fan, and K. B. Letaief, "AoI-minimal trajectory planning and data collection in UAV-assisted wireless powered IoT networks," *IEEE Internet of Things Journal*, vol. 8, no. 2, pp. 1211–1223, 2021.

[5] X. Xu, Q. Wu, L. Qi, W. Dou, S. B. Tsai, and M. Z. A. Bhuiyan, "Trust-aware service offloading for video surveillance in edge computing enabled Internet of vehicles," *IEEE Transactions on Intelligent Transportation Systems*, vol. 22, no. 3, pp. 1787–1796, 2021.

[6] X. Liu, K. Zheng, L. Fu, X.-Y. Liu, X. Wang, and G. Dai, "Energy efficiency of secure cognitive radio networks with cooperative spectrum sharing," *IEEE Transactions on Mobile Computing*, vol. 18, no. 2, pp. 305–318, 2019.

[7] K. Zheng, X.-Y. Liu, X. Liu, and Y. Zhu, "Hybrid overlay-underlay cognitive radio networks with energy harvesting," *IEEE Transactions on Communications*, vol. 67, no. 7, pp. 4669–4682, 2019.

[8] X. Liu, K. Zheng, K. Chi, and Y. -H. Zhu, "Cooperative spectrum sensing optimization in energy-harvesting cognitive radio networks," *IEEE Transactions on Wireless Communications*, vol. 19, no. 11, pp. 7663–7676, 2020.

[9] I. Budhiraja, N. Kumar, and S. Tyagi, "Energy-delay tradeoff scheme for NOMA-based D2D groups with WPCNs," *IEEE Systems Journal*, vol. 15, no. 4, pp. 4768–4779, 2021.

[10] H. Lee, K. -J. Lee, H. Kim, B. Clerckx, and I. Lee, "Resource allocation techniques for wireless powered communication networks with energy storage constraint," *IEEE Transactions on Wireless Communications*, vol. 15, no. 4, pp. 2619–2628, 2016.

[11] D. Song, W. Shin, J. Lee, and H. V. Poor, "Sum-Throughput maximization in NOMA-based WPCN: a cluster-specific beamforming approach," *IEEE Internet of Things Journal*, vol. 8, no. 13, pp. 10543–10556, 2021.

[12] C. Jeong and H. Son, "Cooperative transmission of energy-constrained IOT devices in wireless-powered communication networks," *IEEE Internet of Things Journal*, vol. 8, no. 5, pp. 3972–3982, 2021.

[13] F. K. Ojo, D. O. Akande, and M. F. M. Salleh, "Optimal power allocation in cooperative networks with energy-saving protocols," *IEEE Transactions on Vehicular Technology*, vol. 69, no. 5, pp. 5079–5088, 2020.

[14] T. -T. Nguyen, Q. -V. Pham, V. -D. Nguyen, J. -H. Lee, and Y. -H. Kim, "Resource allocation for energy efficiency in OFDMA-enabled WPCN," *IEEE Wireless Communications Letters*, vol. 9, no. 12, pp. 2049–2053, 2020.

[15] M. Al Samara, I. Bennis, A. Abouaissa, and P. Lorenz, "An efficient outlier detection and classification clustering-based approach for WSN," in *IEEE Global Communications Conference*, pp. 1–6, Madrid, Spain, 2021.

[16] K. Sood, M. R. Nosouhi, N. Kumar, A. Gaddam, B. Feng, and S. Yu, "Accurate detection of IoT sensor behaviors in legitimate, faulty and compromised scenarios," *IEEE Transactions on Dependable and Secure Computing*, 2022.

[17] S. Wang, X. Mao, S. -J. Tang, X. Li, J. Zhao, and G. Dai, "On "movement-assisted connectivity restoration in wireless sensor and actor networks"," *IEEE Transactions on Parallel and Distributed Systems*, vol. 22, no. 4, pp. 687–694, 2011.

[18] V. K. Akram, O. Dagdeviren, and B. Tavli, "A coverage-aware distributedk-connectivity maintenance algorithm for arbitrarily largekin mobile sensor networks," *IEEE/ACM Transactions on Networking*, vol. 30, no. 1, pp. 62–75, 2022.

[19] W. Liu, K. Lu, J. Wang et al., "On the throughput-delay tradeoff in large-scale manets with a generalized i.i.d. mobility model," in *IEEE International Conference on Computer Communications*, pp. 1321–1329, Turin, Italy, 2013.

[20] K. Zheng, X. Liu, B. Wang, H. Zheng, K. Chi, and Y. Yao, "Throughput maximization of wireless-powered communication

networks: an energy threshold approach," *IEEE Transactions on Vehicular Technology*, vol. 70, no. 2, pp. 1292–1306, 2021.

[21] S. Hu, X. Chen, W. Ni, X. Wang, and E. Hossain, "Modeling and analysis of energy harvesting and smart grid-powered wireless communication networks: a contemporary survey," *IEEE Transactions on Green Communications and Networking*, vol. 4, no. 2, pp. 461–496, 2020.

[22] A. D. Polyanin and A. V. Manzhrov, *Handbook of Mathematics for Engineers and Scientists*, Chapman & Hall/CRC Press, LCC, London, U.K./New York, USA, 1st edition, 2007.

[23] S. Gilbert, *Linear Algebra and Its Applications*, Brooks Cole, Boston, USA, 4th edition, 2004.

[24] J. Qin, W. Fu, H. Gao, and W. X. Zheng, "Distributed k-means algorithm and fuzzy c-means algorithm for sensor networks based on multiagent consensus theory," *IEEE Transactions on Cybernetics*, vol. 47, no. 3, pp. 772–783, 2017.

[25] T. Wang, Q. Li, D. J. Bucci, Y. Liang, B. Chen, and P. K. Varshney, "K-medoids clustering of data sequences with composite distributions," *IEEE Transactions on Signal Processing*, vol. 67, no. 8, pp. 2093–2106, 2019.

[26] V. Cohen-Addad, V. Kanade, F. Mallmann-Trenn, and C. Mathieu, "Hierarchical clustering," *Journal of the ACM*, vol. 66, no. 4, pp. 1–42, 2019.